

Article

Theoretical Analysis of Buckling for Functionally Graded Thin Plates with Microstructure Resting on an Elastic Foundation

Jarosław Jędrysiak and Magda Kaźmierczak-Sobińska *

Department of Structural Mechanics, Łódź University of Technology, al. Politechniki 6, 90-924 Łódź, Poland; jarek@p.lodz.pl

* Correspondence: magda.sobinska@wp.pl; Tel.: +48-42-631-3564

Received: 24 July 2020; Accepted: 8 September 2020; Published: 11 September 2020



Abstract: In this paper, the problem of the stability of functionally graded thin plates with a microstructure is presented. To analyse this problem and take into consideration the effect of microstructure, tolerance modelling is used. The tolerance averaging technique allows us to replace the equation with non-continuous, tolerance-periodic, highly oscillating coefficients of the system of differential equations with slowly-varying coefficients, which describes also the effect of the microstructure. As an example, the buckling of a microstructured functionally graded plate band on a foundation is investigated. To obtain results, the tolerance model and the asymptotic model combined together with the Ritz method are used. It is shown that the tolerance model allows us to take into account the effect of microstructure on critical forces.

Keywords: functionally graded thin plate; tolerance modelling; effect of microstructure

1. Introduction

The stability problem of thin functionally graded microstructured plates is considered in this paper. Moreover, these plates can interact with a heterogeneous elastic foundation. It is assumed that on the macrolevel, the plate has functionally graded distributions of properties in planes parallel to the plate midplane, but on the microlevel has a tolerance-periodic structure in these planes, cf. References [1,2]. This structure of the plate can be caused by a proper distribution of geometric properties (a plate thickness) or material properties (mixture/system of various materials). Hence, plates of this kind can be called as *functionally graded* or also as *tolerance-periodic plates*. In such plates, a “basic cell” can be marked, which can be treated as a thin plate, cf. Figure 1, with a fragment of the plate. These adjacent cells are almost identical, but distant ones can be very different.

Functionally graded structures are often described using the known averaging approaches, proposed for periodic media. Some of them can be found in Reference [1]. In the modelling of functionally graded microstructured plates, similar methods can be used. Models based on the asymptotic homogenization approach, cf. Reference [3], can be mentioned, e.g., applied to analyse periodic plates, cf. Reference [4]. To describe different composite media (also periodically microstructured) there are also proposed various other modelling methods, e.g., a homogenization based on microlocal parameters for periodic plates was used in Reference [5]; natural frequencies of thick plates made of orthotropic materials were analysed in Reference [6]; the stability of thin-walled columns with cells was considered in Reference [7]; the dynamic stability of sandwich beams and plates with a core having variable mechanical properties was analysed in References [8–11]; the stability of three-layered annular plates composed of laminated fibre-reinforced composite facings and foam core was investigated in Reference [12]; a torsion of composite beams with a phase made of an auxetic material with a

microstructure was analysed in References [13,14], applying a certain analytical-numerical model based on analytical relations and the finite element method.

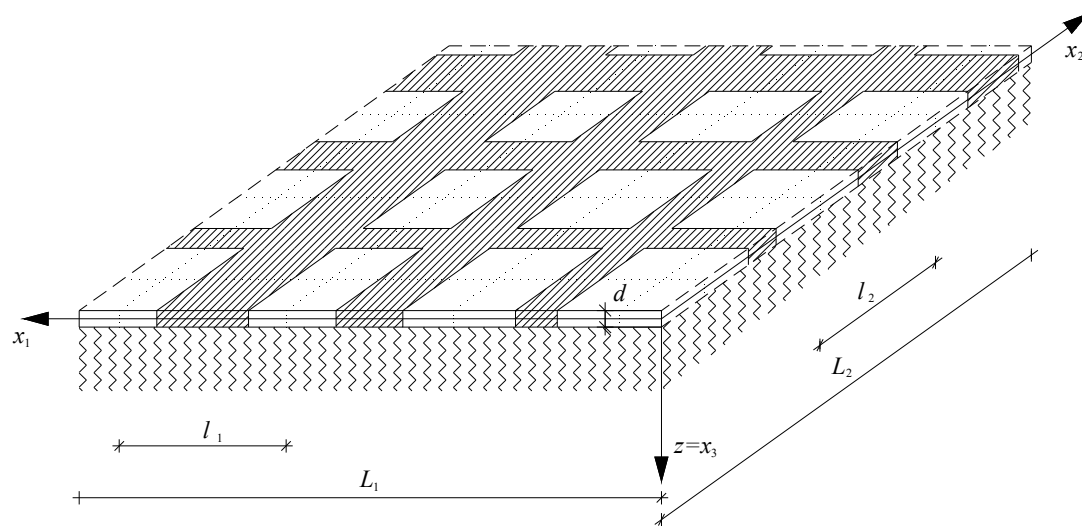


Figure 1. A fragment of a microstructured functionally graded plate (tolerance-periodic plate) on a heterogeneous elastic foundation.

Different theoretical and numerical results of various problems of functionally graded structures can be found in many articles. The higher-order theory for various thermomechanical problems of functionally graded fibre reinforced composites with microstructure was proposed and developed in Reference [15–18]. Applications of the known numerical methods for functionally graded materials were shown in many papers, e.g., the boundary element method was applied to the thermal analysis of composites with fibres in Reference [19]; a certain implementation of the finite element method for functionally graded materials was presented in Reference [20]. The stability of cylindrical shells with functionally graded structure applying Donnell type dynamic stability equations was analysed in Reference [21]. Meshless methods were used to investigate natural frequencies in a few articles, e.g., in Reference [22] for functionally graded plates, and in Reference [23] for sandwich beams with the functionally graded structure of a core. Higher-order plate theories and a collocation method were applied to vibrations of functionally graded plates in Reference [24]. A GDQ solution was proposed in Reference [25] to analyse the free vibration problems of shells. Higher-order deformation theories were applied to analyse thermomechanical problems of functionally graded plates and shells in Reference [26,27]. The statics of doubly-curved functionally graded shells was considered in Reference [28–30]. The non-classical FGM plate model based on the modified couple stress theory was proposed for the thermal buckling of annular functionally graded plates in Reference [31], where the size effect, related to the couple stress theory, was analysed. The influence of the shear correction function in a modal analysis of functionally graded beams was investigated in Reference [32]. An optimization of free vibrations for functionally graded beams was presented in Reference [33]. Free vibrations of thick functionally graded plates were considered in Reference [34], taking into account the effects of normal and shear deformations. A higher-order normal and shear deformable theory of plates was used in Reference [35] for vibrations of rectangular functionally graded plates. Non-linear analysis based on a shear deformation theory for functionally graded plates was presented in Reference [36]. A chaos problem for a rectangular functionally graded plate was investigated in Reference [37]. A strong formulation based on the GDQ technique to finite element method for multilayered plates was proposed in Reference [38], but a strong formulation of isogeometric analysis for composite laminated plates was shown in Reference [39]. A differential quadrature method and a layer-wise theory for composite plates were applied in Reference [40]. A new low-order shell element was used in Reference [41] for shell structures having functionally graded material properties. The differential quadrature method was

applied to analyse different problems of functionally graded shells and, plates e.g., in Reference [42] for natural frequencies of sandwich shells; for dynamic stability of layered shells in Reference [43]. The theory of sinusoidal shear deformation was applied in Reference [44,45] to describe the bending of piezoelectric functionally graded plates on a foundation and to analyse the free vibrations of composite functionally graded polymer nanoplates. The classical laminate plate theory was applied to formulate the semi-analytical method to analyse certain stability and dynamical problems of thin functionally graded plates, cf. Reference [46], or of columns with open/closed cross-sections made of those plates, cf. Reference [47,48]. Free vibrations of thermally loaded functionally graded sandwich plates were investigated using three-dimensional finite element modelling in Reference [49]. The transient behaviors of functionally graded materials plates with the influence of in-plane displacements and of temperature changes were considered in Reference [50] applying a new semi-analytical algorithm. In Reference [51], an analytical method was proposed using the complex variable approach to analyse forces and moments acting on infinite symmetric functionally graded plates with a triangular hole. Love waves propagated in a functionally graded saturated layer resting on a saturated semi-space were considered in Reference [52]. A certain review of modelling methods for plates with functional gradation of material properties is shown in Reference [53]. However, the analysed examples concerned the change of properties along the thickness of the plate, and not in the midplane of the plate as in this paper.

These models are described by governing equations, which usually vanish the effect of microstructure size, cf. Reference [54], and this effect cannot be analysed by these models. However, this effect may be relevant to the overall behaviour of microheterogeneous structures. This can be observed in a few of articles, e.g., a spectral element method was used in Reference [55] to analyse the properties of the vibration bandgap for Mindlin's periodic plates; a centre finite difference method was applied in Reference [56,57] to investigate band gaps of thin periodic plates with or without damping; the differential quadrature element method was used in Reference [58] to analyse flexural wave band gaps in periodic composite plates.

The effect of microstructure size can be also analysed using *the tolerance averaging method*, cf. Reference [2,59,60]. This modelling approach allows us to include this effect in the governing equations, which describe the overall behaviour of media with a microstructure, which can be caused by the distribution of different materials. This method makes it possible to investigate various dynamical, stability, and thermoelastic problems for periodic structures, which can be found in a series of articles. For instance: fluid-saturated periodic grounds were investigated in Reference [61]; the dynamics of periodic plane structures was considered in Reference [62]; the vibrations of wavy-type periodic plates were analysed in Reference [63]; the dynamics of periodic thin plates reinforced by stiffeners was described in Reference [64]; an application for vibrations of medium thickness periodic plates was shown in Reference [65]; a stability of periodic thin plates on a foundation was considered in Reference [66]; the dynamics of thin periodic plates with the microstructure size of an order of the thickness of the plate was analysed in Reference [67]; applications for dynamics and stability of shells with a periodic microstructure were presented in References [68,69]; the nonlinear dynamics of periodic visco-elastic plates was shown in Reference [70]; the geometrically nonlinear dynamics of periodic beams was analysed in Reference [71,72]; the vibrations of three-layered periodic plates were considered in Reference [73]; an analysis of free vibrations for thin periodic plates having uncertain material properties was presented in Reference [74].

The tolerance modelling approach can be also successfully applied to consider various problems of thermomechanics for functionally graded structures. For instance: investigations of dynamics for longitudinally graded plates were presented in References [75–77]; vibrations of thin functionally graded plates with the size of the microstructure of an order of the thickness of the plate were analysed in Reference [78]; vibrations of thin transversally graded plates with the thickness smaller than the microstructure size were shown in Reference [2,79,80]; dynamics of a thin-walled structure with a system of ribs was presented in Reference [81,82]; heat distribution of composite cylindrical conductors

having non-uniform microstructure was analysed in Reference [83,84]; problems of thermoelasticity in transversally graded laminates were considered in Reference [85]; dynamics of thin functionally graded microstructured shells was presented in Reference [86–88].

On the basis of the literature, it can be noted that the vast majority of the analysed mechanical problems concern layered functionally graded beams, plates, shells, or such structures with functional gradation along the thickness. Only a relatively small part of the work is devoted to the mechanical problems of structures with functional graded properties along the length, i.e., in the plane of the plate, in the shell surface, and along the longitudinal axis of the beam/bar. It seems that most of them show models based on the tolerance modelling method, cf. References [2,60,75–82,86–88], and between them References [76,88] present stability problems of functionally graded plates or shells.

In this contribution, the *tolerance model equations* of the thin functionally graded microstructured plates with in-plane forces, taking into account the effect of microstructure size, are presented. Moreover, in order to evaluate the obtained results, the asymptotic model equations known from the literature were introduced. These equations of both the models are also applied to analyse the buckling of a simply supported microstructured plate band. To obtain formulas of critical forces, the Ritz method is applied. In this work, an application of the tolerance model to the analysis of critical forces of thin functionally graded plate bands on an elastic foundation is shown, including microstructure size, an elasticity coefficient of the foundation, and different distributions of properties along the length of the plate band. In the presented example, there are considered functionally graded plate bands with a material microstructure related to the proposed different distribution of two materials.

2. Modelling Approach

2.1. Modelling Preliminaries

Denote by $Ox_1 \times x_3$ the orthogonal Cartesian coordinate system. Let subscripts i, k, l run over 1,2,3, but α, β, γ run over 1,2. Denote also $\mathbf{x} \equiv (x_1, x_2)$, $z \equiv x_3$. Let the region of the undeformed plate be denoted by $\Omega \equiv \{(\mathbf{x}, z) : -d/2 \leq z \leq d/2, \mathbf{x} \in \Pi\}$, where Π is the plate midplane and $d(\cdot)$ is the plate thickness. Derivatives of x_α are denoted by δ_α and also $\delta_{\alpha\dots\delta} \equiv \delta_\alpha\dots\delta_\delta$. Let $\Delta \equiv [-l_1/2, l_1/2] \times [-l_2/2, l_2/2]$ be the “basic cell” on Ox_1x_2 , with l_α as its length dimensions along the x_α -axis. The diameter of cell Δ is denoted by $l \equiv [(l_1)^2 + (l_2)^2]^{1/2}$ and is called the *microstructure parameter*. It is assumed that this parameter satisfies condition $d_{\max} \ll l \ll \min(L_1, L_2)$. Thickness $d(\cdot)$ can be a tolerance-periodic function in \mathbf{x} and also elastic moduli $a_{ijlm} = a_{ijlm}(\cdot, z)$ can be tolerance-periodic functions in \mathbf{x} and even functions in z . Denote $c_{\alpha\beta\gamma\delta} \equiv a_{\alpha\beta\gamma\delta} - a_{\alpha\beta 33}a_{\gamma\delta 33}(a_{3333})^{-1}$, $c_{\alpha 3\gamma 3} \equiv a_{\alpha 3\gamma 3} - a_{\alpha 333}a_{33\gamma 3}(a_{3333})^{-1}$, where $a_{\alpha\beta\gamma\delta}$, $a_{\alpha\beta 33}$, $a_{\alpha 3\gamma 3}$, a_{3333} are the non-zero components of the elastic moduli tensor. We also assume that properties of an elastic foundation of the Winkler’s type are described by a tolerance-periodic function in \mathbf{x} —a Winkler’s coefficient k . Let $w(\mathbf{x})$ ($\mathbf{x} \in \Pi$) be a plate deflection and p be total loadings in the z -axis direction.

Denoting bending stiffnesses $d_{\alpha\beta\gamma\delta}$ of the plate, being tolerance-periodic functions in \mathbf{x} , in the form:

$$d_{\alpha\beta\gamma\delta}(\mathbf{x}) \equiv \int_{-d/2}^{d/2} c_{\alpha\beta\gamma\delta}(\mathbf{x}, z) z^2 dz, \quad (1)$$

from the Kirchhoff-type plates theory assumptions used to functionally graded plates the lagrangean can be formulated:

$$\Lambda = -\frac{1}{2} (d_{\alpha\beta\gamma\delta} \partial_{\alpha\beta} w \partial_{\gamma\delta} w + \partial_\alpha w n_{\alpha\beta} \partial_\beta w + k w w) + p w, \quad (2)$$

for which the Euler-Lagrange equation can be written:

$$-\partial_{\alpha\beta} \frac{\partial \Lambda}{\partial \partial_{\alpha\beta} w} + \partial_\alpha \frac{\partial \Lambda}{\partial (\partial_\alpha w)} - \frac{\partial \Lambda}{\partial w} = 0. \quad (3)$$

Combining Equations (2) and (3), the known fourth-order partial differential equation for deflection $w(\mathbf{x})$ is obtained:

$$\partial_{\alpha\beta}(\partial_{\alpha\beta\gamma\delta}\partial_{\gamma\delta}w) - \partial_{\beta}(n_{\alpha\beta}\partial_{\alpha}w) + kw = p. \quad (4)$$

Equation (4) has non-continuous, highly oscillating, tolerance-periodic functional coefficients.

2.2. Introductory Concepts of the Tolerance Modelling

Certain concepts defined in References [2,60] are applied in the modelling. Hence, some of them are given below, but for functionally graded plates they were also shown in Reference [2,79,80].

Let $\Delta(\mathbf{x}) \equiv \mathbf{x} + \Delta$ be a cell at $\mathbf{x} \in \Pi_{\Delta}$, $\Pi_{\Delta} = \{\mathbf{x} \in \Pi: \Delta(\mathbf{x}) \subset \Pi\}$. The *averaging operator* for an integrable function f is defined by

$$\langle f \rangle(\mathbf{x}) = \frac{1}{l_1 l_2} \int_{\Delta(\mathbf{x})} f(y_1, y_2) dy_1 dy_2, \quad \mathbf{x} \in \Pi. \quad (5)$$

The averaged value calculated from (5) of function f , being a tolerance-periodic in \mathbf{x} , is a slowly-varying function in \mathbf{x} .

Let $\partial^k f$ denote the k -th gradient of function $f = f(\mathbf{x})$, $\mathbf{x} \in \Pi$, $k = 0, 1, \dots, \alpha$, ($\alpha \geq 0$); $\partial^0 f \equiv f$; and $\tilde{f}^{(k)}(\cdot, \cdot)$ be a function defined in $\Pi \times R^m$. Moreover, the parameter δ is small, $\delta < 1$, called the *tolerance parameter*. This parameter is related to and dependent on every problem under consideration.

Function $f \in H^{\alpha}(\Pi)$ is the *tolerance-periodic function*, $f \in TP_{\delta}^{\alpha}(\Pi, \Delta)$, if for $k = 0, 1, \dots, \alpha$, the following conditions are satisfied:

$$\begin{aligned} & (\forall \mathbf{x} \in \Pi) (\exists \tilde{f}^{(k)}(\mathbf{x}, \cdot) \in H^0(\Delta)) [\|\partial^k f|_{\Pi_{\Delta}}(\cdot) - \tilde{f}^{(k)}(\mathbf{x}, \cdot)\|_{H^0(\Pi, \Delta)} \leq \delta], \\ & (1) \int_{\Delta(\cdot)} \tilde{f}^{(k)}(\cdot, \mathbf{z}) d\mathbf{z} \in C^0(\overline{\Pi}), \end{aligned}$$

where function $\tilde{f}^{(k)}(\mathbf{x}, \cdot)$ is the *periodic approximation of $\partial^k f$ in $\Delta(\mathbf{x})$* , $\mathbf{x} \in \Pi$, $k = 0, 1, \dots, \alpha$.

Function $F \in H^{\alpha}(\Pi)$ is the *slowly-varying function*, $F \in SV_{\delta}^{\alpha}(\Pi, \Delta)$, if

$$\begin{aligned} & F \in TP_{\delta}^{\alpha}(\Pi, \Delta), \\ & (\forall \mathbf{x} \in \Pi) [\tilde{f}^{(k)}(\mathbf{x}, \cdot)|_{\Delta(\mathbf{x})} = \partial^k F(\mathbf{x}), \quad k = 0, \dots, \alpha]. \end{aligned}$$

Function $\varphi \in H^{\alpha}(\Pi)$ is the *highly oscillating function*, $\varphi \in HO_{\delta}^{\alpha}(\Pi, \Delta)$, if

$$\begin{aligned} & \varphi \in TP_{\delta}^{\alpha}(\Pi, \Delta), \\ & (\forall \mathbf{x} \in \Pi) [\tilde{\varphi}^{(k)}(\mathbf{x}, \cdot)|_{\Delta(\mathbf{x})} = \partial^k \varphi(\mathbf{x}), \quad k = 0, 1, \dots, \alpha]. \\ & \forall F \in SV_{\delta}^{\alpha}(\Pi, \Delta) \exists f \equiv \varphi F \in TP_{\delta}^{\alpha}(\Pi, \Delta) \quad \tilde{f}^{(k)}(\mathbf{x}, \cdot)|_{\Delta(\mathbf{x})} = F(\mathbf{x}) \partial^k \varphi(\mathbf{x})|_{\Delta(\mathbf{x})}, \quad k = 1, \dots, \alpha. \end{aligned}$$

For $k = 0$ let us denote $\tilde{f} \equiv \tilde{f}^{(0)}$. Moreover, for the plates under consideration, the parameter α is restricted to 2, $\alpha = 2$.

Let $h(\cdot)$ be a highly oscillating function, defined on Π , $h \in HO_{\delta}^2(\Pi, \Delta)$, continuous together with gradient $\delta^1 h$. Gradient $\delta^2 h$ is a piecewise continuous and bounded. Function $h(\cdot)$ is the *fluctuation shape function* of the 2-nd kind, $FS_{\delta}^2(\Pi, \Delta)$, if it depends on l as a parameter and the conditions hold:

$$\begin{aligned} & \delta^k h \in O(l^{\alpha-k}) \quad \text{for } k = 0, 1, \dots, \alpha, \alpha = 2, \delta^0 h \equiv h, \\ & \langle h \rangle(\mathbf{x}) \approx 0 \quad \text{for every } \mathbf{x} \in \Pi_{\Delta}. \end{aligned}$$

2.3. Tolerance Modelling Assumptions

Applying the introductory concepts, the modelling assumptions can be formulated, cf. References [2,79,80].

The micro-macro decomposition is the first assumption, introduced in the form:

$$w(\mathbf{x}) = U(\mathbf{x}) + h^A(\mathbf{x})Q^A(\mathbf{x}), \quad A = 1, \dots, M, \quad \mathbf{x} \in \Pi, \quad (6)$$

where $U(\cdot), Q^A(\cdot) \in SV_\delta^2(\Pi, \Delta)$, i.e., they are slowly-varying functions of the 2-nd kind. Functions $U(\cdot)$ and $Q^A(\cdot)$ are new basic kinematic unknowns, named *the macrodeflection* and *the fluctuation amplitudes*, respectively; $h^A(\cdot)$ are the known fluctuation shape functions, satisfying the condition $\langle h^A h^B \rangle \approx 0, A, B = 1, \dots, M$.

The tolerance averaging approximation is the second assumption, in which terms $O(\delta)$ are assumed to be negligibly small, e.g., for $f \in TP_\delta^2(\Pi, \Delta), F \in SV_\delta^2(\Pi, \Delta), h^A \in FS_\delta^2(\Pi, \Delta)$, in:

$$\begin{aligned} \langle f \rangle(\mathbf{x}) &= \langle \bar{f} \rangle(\mathbf{x}) + O(\delta), \\ \langle fF \rangle(\mathbf{x}) &= \langle f \rangle(\mathbf{x})F(\mathbf{x}) + O(\delta), \\ \langle f\partial_\alpha(h^A F) \rangle(\mathbf{x}) &= \langle f\partial_\alpha h^A \rangle(\mathbf{x})F(\mathbf{x}) + O(\delta). \end{aligned} \quad (7)$$

The in-plane forces restriction is the third assumption, which allows us to neglect terms involving fluctuating parts of in-plane forces in comparing to terms with averaged parts, i.e.:

$$\begin{aligned} n_{\alpha\beta}(\mathbf{x}) &= N_{\alpha\beta}(\mathbf{x}) + \tilde{n}_{\alpha\beta}(\mathbf{x}), \\ N_{\alpha\beta} &= \langle n_{\alpha\beta} \rangle, \quad \langle \tilde{n}_{\alpha\beta} \rangle = 0, \end{aligned} \quad (8)$$

where $N_{\alpha\beta}(\cdot) \in SV_\delta^2(\Pi, \Delta)$ and $\tilde{n}_{\alpha\beta}(\cdot) \in TP_\delta^2(\Pi, \Delta)$ are *averaged* and *fluctuating part of in-plane forces*, respectively.

2.4. The Outline of the Tolerance Modelling Procedure

Following References [2] or [79,80], the modelling procedure is briefly introduced. The formulation of the lagrangean Λ in the form (2) is the starting point of the modelling. From combining the Euler-Lagrange equation (3) with the lagrangean (2), the governing equation of the plate is derived in the form (4).

Applying tolerance modelling to the lagrangean (2), there are three steps. In the first, the micro-macro decomposition (6) is substituted into (2); in the second, the averaging operator (5) is used to obtain averaged functional; and in the third, the restriction (8) and the approximation (7) are used for this functional. This leads to the tolerance averaged lagrangean $\langle \mathcal{L}_h \rangle$ in the form:

$$\begin{aligned} \langle \Lambda_h \rangle = - & \frac{1}{2} \left\{ \left(\langle d_{\alpha\beta\gamma\delta} \rangle \partial_{\alpha\beta} U + 2 \langle d_{\alpha\beta\gamma\delta} \partial_{\alpha\beta} h^B \rangle Q^B \right) \partial_{\gamma\delta} U + \right. \\ & + \partial_\alpha U \langle n_{\alpha\beta} \rangle \partial_\beta U + \langle k \rangle UU + 2U \langle kh^B \rangle Q^B + \langle kh^A h^B \rangle Q^A Q^B + \\ & \left. + \left(\langle d_{\alpha\beta\gamma\delta} \partial_{\alpha\beta} h^A \partial_{\gamma\delta} h^B \rangle + \langle n_{\alpha\beta} \partial_\alpha h^A \partial_\beta h^B \rangle \right) Q^A Q^B \right\} + \langle p \rangle U + \langle ph^A \rangle Q^A. \end{aligned} \quad (9)$$

From the principle of stationary action applied to (9) the averaged Euler-Lagrange equations for $U(\cdot, t)$ and $Q^A(\cdot, t)$ take the following form:

$$\begin{aligned} -\partial_{\alpha\beta} \frac{\partial \langle \Lambda_h \rangle}{\partial \partial_{\alpha\beta} U} + \partial_\alpha \frac{\partial \langle \Lambda_h \rangle}{\partial (\partial_\alpha U)} - \frac{\partial \langle \Lambda_h \rangle}{\partial U} &= 0, \\ -\frac{\partial \langle \Lambda_h \rangle}{\partial Q^A} &= 0. \end{aligned} \quad (10)$$

2.5. Governing Equations

2.5.1. The Tolerance Model Equations

Substituting the tolerance averaged lagrangean (9) to the averaged Euler-Lagrange equations (10), introducing denotations:

$$\begin{aligned} D_{\alpha\beta\gamma\delta} &\equiv \langle d_{\alpha\beta\gamma\delta} \rangle, & D_{\alpha\beta}^A &\equiv \langle d_{\alpha\beta\gamma\delta} \partial_{\gamma\delta} h^A \rangle, & D^{AB} &\equiv \langle d_{\alpha\beta\gamma\delta} \partial_{\alpha\beta} h^A \partial_{\gamma\delta} h^B \rangle, \\ K &\equiv \langle k \rangle, & K^A &\equiv l^{-2} \langle kh^A \rangle, & K^{AB} &\equiv l^{-4} \langle kh^A h^B \rangle, \\ H_{\alpha\beta}^{AB} &\equiv l^{-2} \langle \partial_{\alpha\beta} h^A h^B \rangle, & P &\equiv \langle p \rangle, & P^A &\equiv l^{-2} \langle ph^A \rangle, \end{aligned} \quad (11)$$

and after some manipulations the following equations for $U(\cdot)$ and $Q^A(\cdot)$ are obtained:

$$\begin{aligned} \underline{\partial_{\alpha\beta}(D_{\alpha\beta\gamma\delta}\partial_{\gamma\delta} U + D_{\alpha\beta}^A Q^A) - \partial_\alpha(N_{\alpha\beta}\partial_\beta U) + KU + l^2\underline{K^A Q^A} = P}, \\ \underline{D_{\gamma\delta}^A \partial_{\gamma\delta} U + D^{AB} Q^B - l^2 N_{\alpha\beta} H_{\alpha\beta}^{AB} Q^B + l^2 \underline{K^A U} + l^4 \underline{K^{AB} Q^B} = l^2 \underline{P^A}}, \end{aligned} \quad (12)$$

which stand for the system of the partial differential equations. All coefficients of Equations (12) are slowly-varying functions in x in contrast to Equation (2), having non-continuous, highly oscillating, and tolerance-periodic coefficients. The underlined terms in the above equations are dependent of the microstructure parameter l . Equations (12) with micro-macro decomposition (6) describe the stability of plates under consideration in the framework of the *tolerance model of thin microstructured functionally graded plates*. These governing equations involve coefficients (underlined) describing the effect of microstructure size in these plates. Hence, this model allows us to analyse this effect in the stability problems of the considered plates. The basic kinematic unknowns $U, Q^A, A = 1, \dots, M$, are slowly-varying functions in x . Boundary conditions can be only formulated for the *macrodeflection* U , but not for the *fluctuation amplitudes* Q^A .

2.5.2. The Asymptotic Model Equations

Results obtained in the framework of the tolerance model can be evaluated using an approximate model, in which the effect of microstructure size is neglected. Using the proper asymptotic modelling procedure, cf. References [60,78,79], or after neglecting the underlined terms in Equation (12), the following equation can be written:

$$\partial_{\alpha\beta} \left(D_{\alpha\beta\gamma\delta}^{eff} \partial_{\gamma\delta} U \right) - \partial_\alpha (N_{\alpha\beta} \partial_\beta U) + KU = P, \quad (13)$$

with the effective averaged bending stiffness defined by:

$$D_{\alpha\beta\gamma\delta}^{eff} \equiv D_{\alpha\beta\gamma\delta} - D_{\alpha\beta}^A (D^{AB})^{-1} D_{\gamma\delta}^B. \quad (14)$$

Equation (13) represents the *asymptotic model of thin microstructured functionally graded plates*, which neglects the effect of microstructure size. In comparison with Equation (2), which has non-continuous, tolerance-periodic coefficients, Equation (13) has smooth, slowly-varying coefficients. It should be noted that only one differential Equation (13) for the macrodeflection U , with the effective stiffness (14), is obtained.

3. Application—A Buckling Problem of Simply Supported Functionally Graded Plate Bands

3.1. Introduction

A buckling of a thin plate band with span L along the x_1 -axis is considered as an example. Thus, the loading p is vanished; $p = 0$. It is assumed that a material structure of the plate band is functionally graded along its span, cf. Figure 2. The material properties of the plate are independent of the x_2 -coordinate, hence the stability problem under consideration is treated as independent of the x_2 -coordinate too.

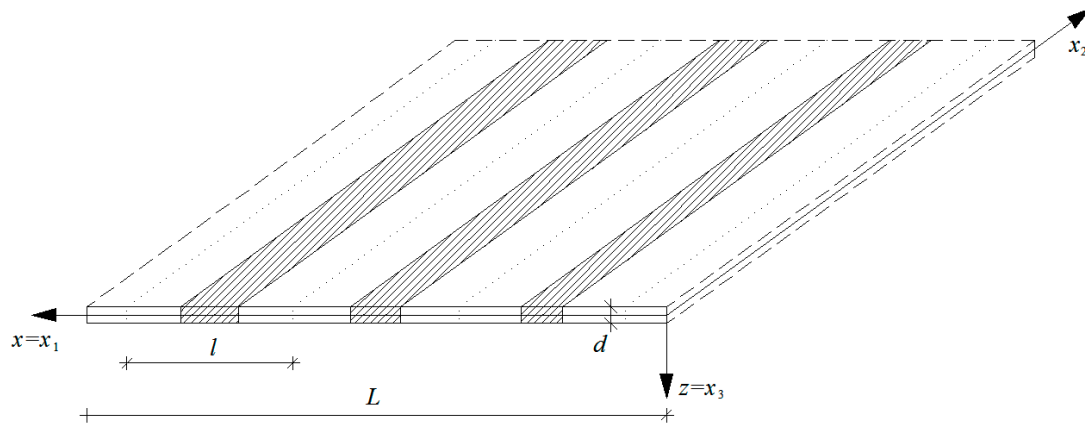


Figure 2. A part of a microstructured functionally graded plate band.

Let $x = x_1, z = x_3, x \in [0, L], z \in [-d/2, d/2]$, where d is a constant plate thickness, and $\delta \equiv \delta_1$. Thus, for this plate, the basic cell is defined as $\Delta \equiv [-l/2, l/2]$ in the interval $\Xi \equiv [0, L]$, and l is the length of this cell, $l \ll L$. Moreover, a cell with a centre at $x \in [0, L]$ is denoted by $\Delta(x) \equiv [x - l/2, x + l/2]$.

It is assumed that the plate band is made of two-component elastic isotropic materials, described by Young's moduli E' , E'' , and Poisson's ratios ν' , ν'' , respectively. These components are perfectly bonded on interfaces. Let us assume that $E(\cdot)$ is a tolerance-periodic function in x , $E(\cdot) \in TP_\delta^0(\Xi, \Delta)$, but Poisson's ratio $\nu \equiv \nu' = \nu''$ is constant. The material structure of the plate band can be treated as functionally graded on the macro-scale, and at the same time tolerance-periodic on the micro-scale along the x -axis if the condition $E' \neq E''$ is satisfied. Moreover, it is assumed that the considered plate band rests on an elastic foundation described by a constant Winkler's coefficient k .

Let the following function describe the Young's modulus of the plate band:

$$E(x, y) = \begin{cases} E', & \text{for } y \in ((1 - \gamma(x))l/2, (1 + \gamma(x))l/2), \\ E'', & \text{for } y \in [0, (1 - \gamma(x))l/2] \cup [(1 + \gamma(x))l/2, l], \end{cases} \quad (15)$$

with $\gamma(x)$, $x \in \Xi = [0, L]$, as a distribution function of material properties, cf. Figure 3.

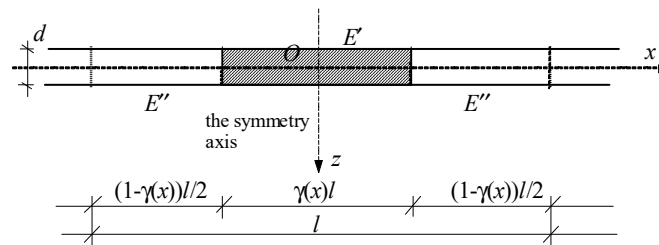


Figure 3. A cell of the microstructured functionally graded plate band.

In the considerations, let us assume only one fluctuation shape function, i.e., $A = M = 1$. Hence, denote $h \equiv h^1$, $Q \equiv Q^1$. Micro-macro decomposition (6) of the field $w(x)$ takes the form:

$$w(x) = U(x) + h(x)Q(x), \quad (16)$$

where $U(\cdot)$, $Q(\cdot) \in SV_\delta^2(\Xi, \Delta)$, $h(\cdot) \in FS_\delta^2(\Xi, \Delta)$.

For the cell assumed in the form shown in Figure 3, the periodic approximation of the fluctuation shape function $h(x)$ can have the form:

$$\tilde{h}(x, y) = l^2 \cos(2\pi y/l), \quad y \in \Delta(x), \quad x \in \Xi. \quad (17)$$

Derivatives $\partial\tilde{h}$, $\partial\partial\tilde{h}$ of the above function take the form:

$$\partial h(y) = -2\pi l \sin(2\pi y/l), \quad \partial\partial h(y) = -4\pi^2 \cos(2\pi y/l). \quad (18)$$

Let us assume that the in-plane forces are only along the x -axis. Hence, $N_{12} = N_{21} = N_{22} = 0$, $N_{11} \neq 0$. Denote also $N = -N_{11}$. Now, tolerance model Equations (12) of the considered plate band have the form:

$$\begin{aligned} \partial\partial(D_{1111}\partial\partial U + D_{11}^1 Q) + \partial(N\partial U) + KU + l^2 K^1 Q &= 0, \\ D_{11}^1 \partial\partial U + D^{11} Q + \underline{l^2 NH_{11}^{11} Q} + \underline{l^2 K^1 U} + \underline{l^4 K^{11} Q} &= 0. \end{aligned} \quad (19)$$

Equation (19) describes a stability problem of the thin microstructured functionally graded plate band in the framework of the tolerance model.

Moreover, for the considered plate band of Equation (13) takes the form:

$$\partial\partial(D_{1111}^{eff}\partial\partial U) + \partial(N\partial U) + KU = 0, \quad (20)$$

with the effective bending stiffness (14):

$$D_{1111}^{eff} \equiv D_{1111} - D_{11}^1 (D^{11})^{-1} D_{11}^1. \quad (21)$$

Equation (20) describes a stability problem of this plate band in the framework of the asymptotic model. Equations (19) and (20) have slowly-varying functional coefficients.

3.2. The Application of the Ritz Method

Since coefficients of Equations (19) and (20) are slowly-varying functions in x , it is difficult to find analytical solutions of them. Hence, formulas of critical forces of plates under consideration can be found applying the known Ritz method, cf. [2,78–80]. In this method, formulas of the maximal strain energy W_{max} should be determined.

For the simply supported plate band, the solution to Equations (19) and (20) can be assumed as:

$$U(x) = A_U \sin(\alpha x), \quad Q(x) = A_Q \sin(\alpha x), \quad (22)$$

where: A_U and A_Q are amplitudes of the macrodeflection and the fluctuation amplitude, respectively; α is a wave number, $\alpha = m\pi/L$, with L as the length of the plate band, m as the number of halfwaves of buckling ($m = 1, 2, 3, \dots$).

Moreover, denotations of coefficients are introduced:

$$\begin{aligned} \breve{B} &= \frac{d^3}{12(1-\nu^2)} \int_0^L \{E''[1 - \tilde{\gamma}(x)] + \tilde{\gamma}(x)E'\} \sin^2(\alpha x) dx, & \bar{B} &= \frac{\pi d^3}{3(1-\nu^2)} (E' - E'') \int_0^L \sin(\pi\tilde{\gamma}(x)) \sin^2(\alpha x) dx, \\ \hat{B} &= \frac{(\pi d)^3}{3(1-\nu^2)} \int_0^L \{(E' - E'')[2\pi\tilde{\gamma}(x) + \sin(2\pi\tilde{\gamma}(x))] + 2\pi E''\} \sin^2(\alpha x) dx, \\ G &= \int_0^L \cos^2(\alpha x) dx, & \bar{G} &= 2\pi^2 \int_0^L \sin^2(\alpha x) dx, & \breve{K} &= k \int_0^L \sin^2(\alpha x) dx, & \bar{K} &= \frac{1}{2} k \int_0^L \sin^2(\alpha x) dx. \end{aligned} \quad (23)$$

Using denotations (23) the maximal strain energy W_{max} by the tolerance model takes the form:

$$W_{max} = \frac{1}{2} [(\breve{B}(A_U)^2 \alpha^2 - 2\bar{B}A_U A_Q - N(A_U)^2 G) \alpha^2 + \breve{K}(A_U)^2 + (\hat{B} + l^4 \bar{K} - l^2 N \bar{G})(A_Q)^2]. \quad (24)$$

Applying the conditions of the Ritz method to Equation (24):

$$\frac{\partial W_{max}}{\partial A_U} = 0, \quad \frac{\partial W_{max}}{\partial A_Q} = 0, \quad (25)$$

after some manipulations, the following formulas are obtained:

$$\begin{aligned} N_- &\equiv \frac{\bar{G}[(\alpha l)^2 \bar{B} + l^2 \alpha^{-2} \bar{K}] + G(\hat{B} + l^4 \bar{K})}{2G\bar{l}^2} - \frac{\sqrt{\left\{\bar{G}[\bar{B}(\alpha l)^2 + l^2 \alpha^{-2} \bar{K}] - G(\hat{B} + l^4 \bar{K})\right\}^2 + 4(\alpha l)^2 G\bar{B}^2}}{2G\bar{l}^2}, \\ N_+ &\equiv \frac{\bar{G}[(\alpha l)^2 \bar{B} + l^2 \alpha^{-2} \bar{K}] + G(\hat{B} + l^4 \bar{K})}{2G\bar{l}^2} + \frac{\sqrt{\left\{\bar{G}[\bar{B}(\alpha l)^2 + l^2 \alpha^{-2} \bar{K}] - G(\hat{B} + l^4 \bar{K})\right\}^2 + 4(\alpha l)^2 G\bar{B}^2}}{2G\bar{l}^2}, \end{aligned} \quad (26)$$

of the lower N_- and, so-called, the higher N_+ critical forces, respectively, in the framework of the tolerance model.

The problem of buckling analysed in the framework of the asymptotic model using the Ritz method leads to the following formula:

$$N_0 \equiv \alpha^2 \frac{\bar{B}\hat{B} - \bar{B}^2}{G\hat{B}} + \alpha^{-2} \frac{K}{G}, \quad (27)$$

of the lower critical force N_0 .

It can be noted that both the tolerance model and the asymptotic model allow us to analyse the problem of buckling for the plate bands under consideration using formulas of the lower (fundamental) critical force (N_- , N_0), but the tolerance model leads also to the formula of the so-called higher critical force (N_+). However, in this paper, considerations are restricted only to the lower critical forces.

3.3. Results

Some numerical results will be calculated for four distribution functions of material properties $\gamma(x)$, in which approximations $\tilde{\gamma}(x)$ are assumed in the form:

$$\begin{aligned} \tilde{\gamma}(x) &= \sin^2(\pi x/L), \\ \tilde{\gamma}(x) &= \cos^2(\pi x/L), \\ \tilde{\gamma}(x) &= (x/L)^2, \\ \tilde{\gamma}(x) &= \sin(\pi x/L), \end{aligned} \quad (28)$$

and will be compared with results for the periodic plate band describing by the constant distribution function:

$$\tilde{\gamma}(x) = \gamma = 0.5, \quad (29)$$

and also for the homogeneous plate band for $\gamma = 0$ (the Young's modulus of the material for the whole plate is E'') and $\gamma = 1$ (the Young's modulus of the material for the whole plate is E').

Let us introduce dimensionless forces ratios given by:

$$n_- \equiv \frac{12(1-\nu^2)}{E'L} N_-, \quad n_0 \equiv \frac{12(1-\nu^2)}{E'L} N_0, \quad (30)$$

for fundamental critical forces N_-, N_0 , described by (26)₁, (27), respectively.

Moreover, the elastic foundation can be described by dimensionless parameter related to the Winkler's coefficient in the following form:

$$\kappa = 12(1-\nu^2)kd(E')^{-1}. \quad (31)$$

Some results calculated by Formula (30) are shown in Figures 4–10. These all plots are made for the Poisson's ratio $\nu = 0.3$. Diagrams in Figures 4–7 and Figure 10 are for the number of halfwaves of buckling assumed $m = 1$.

In Figures 4–7 there are shown plots of the dimensionless forces ratios n_-/n_0 versus the dimensionless microstructure parameter $l/L \in (0, 0.1]$ for four functionally graded plate bands with the distribution functions of material properties $\gamma(x)$ given by: (28)₁—curves no. 1, (28)₂—curves no. 2,

(28)₃—curves no. 3, (28)₄—curves no. 4; and for the periodic plate band with $\gamma = 0.5$, (29), curves no. 5. Plots in Figures 4 and 6 are for the ratio $E''/E' = 0.3$; in Figures 5 and 7—for $E''/E' = 0.5$. Results in Figures 4 and 5 are obtained for $d/L = 0.01$, but in Figures 6 and 7—for $d/L = 0.001$. Figures 4–7, marked by (a), show curves for the parameter $\kappa = 10^{-4}$, but marked by (b) show curves for the parameter $\kappa = 10^{-6}$.

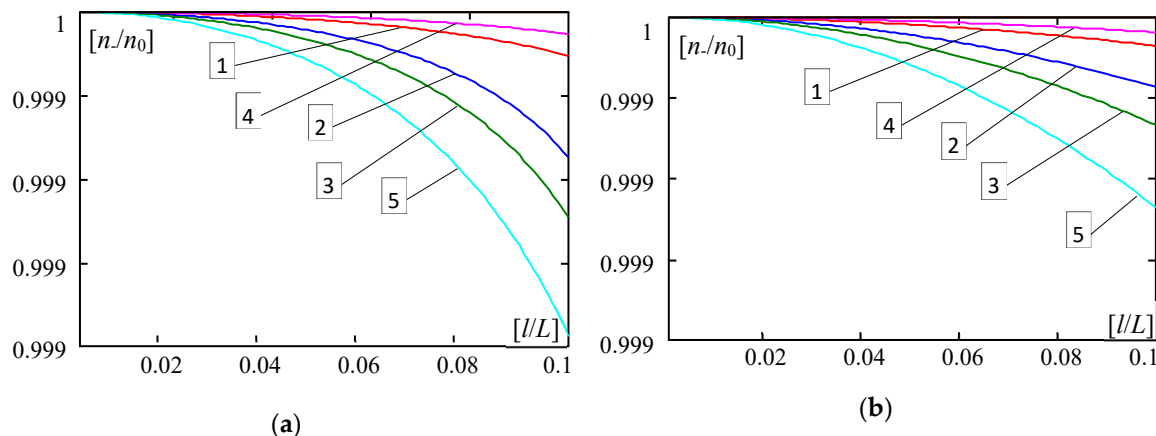


Figure 4. Values of ratios $n./n_0$ versus l/L ($E''/E' = 0.3$, $d/L = 0.01$, $m = 1$). (a) For $\kappa = 0.0001$; (b) For $\kappa = 0.000001$. (1— γ by (28)₁, 2— γ by (28)₂, 3— γ by (28)₃, 4— γ by (28)₄, 5— γ by (29)).

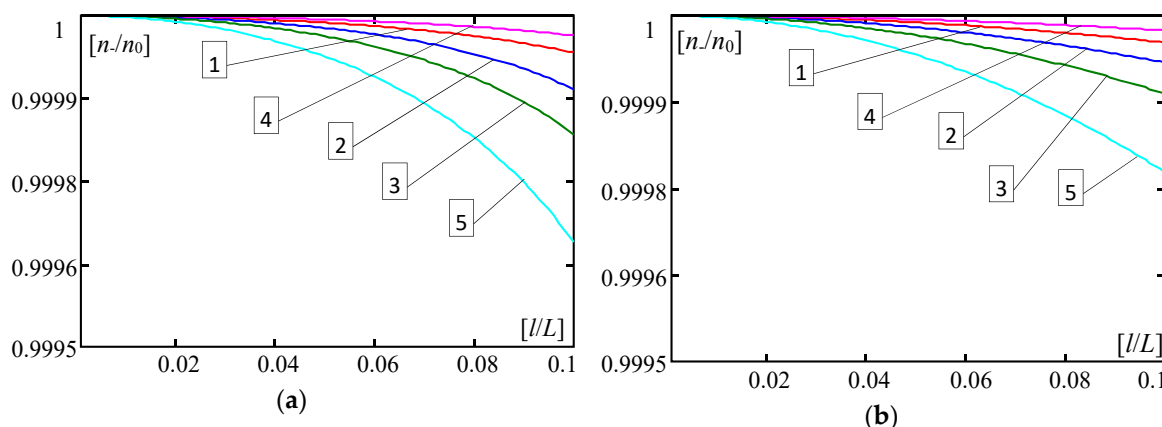


Figure 5. Values of ratios $n./n_0$ versus l/L ($E''/E' = 0.5$, $d/L = 0.01$, $m = 1$). (a) For $\kappa = 0.0001$; (b) For $\kappa = 0.000001$. (1— γ by (28)₁, 2— γ by (28)₂, 3— γ by (28)₃, 4— γ by (28)₄, 5— γ by (29)).

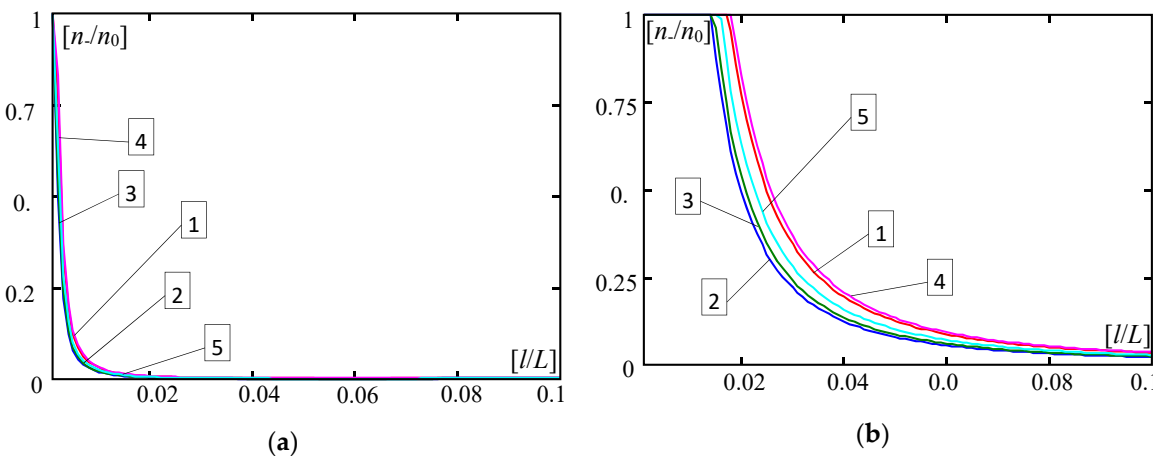


Figure 6. Values of ratios $n./n_0$ versus l/L ($E''/E' = 0.3$, $d/L = 0.001$, $m = 1$). (a) For $\kappa = 0.0001$; (b) For $\kappa = 0.000001$. (1— γ by (28)₁, 2— γ by (28)₂, 3— γ by (28)₃, 4— γ by (28)₄, 5— γ by (29)).

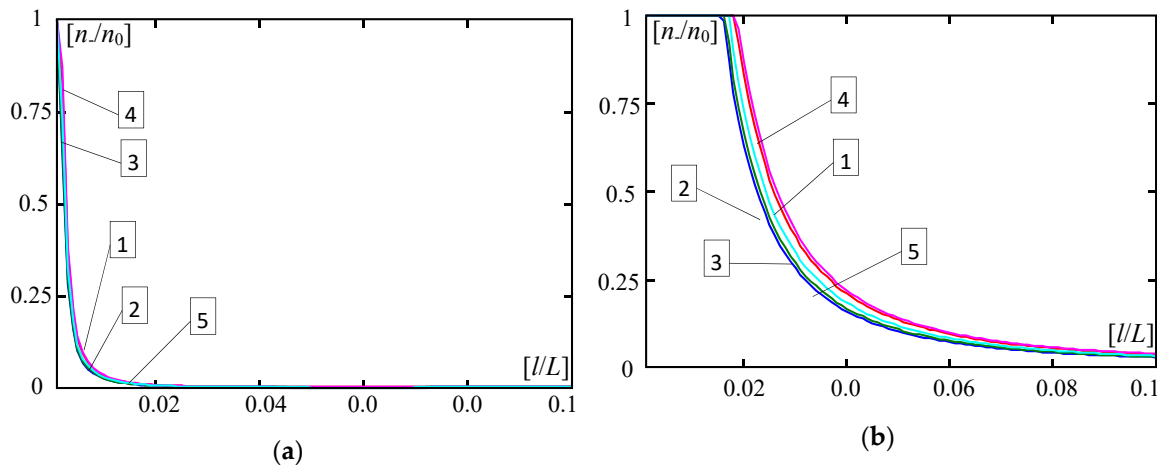


Figure 7. Values of ratios n/n_0 versus l/L ($E''/E' = 0.5$, $d/L = 0.001$, $m = 1$). (a) For $\kappa = 0.0001$; (b) For $\kappa = 0.000001$. (1— γ by (28)₁, 2— γ by (28)₂, 3— γ by (28)₃, 4— γ by (28)₄, 5— γ by (29)).

Figures 8 and 9 present diagrams of the dimensionless forces ratios n, n_0 versus the number m of halfwaves of buckling. They are made for ratios: $d/L = 0.01$, $l/L = 0.1$, $\kappa = 10^{-4}$ (Figure 8); $d/L = 0.002$, $l/L = 0.02$, $\kappa = 10^{-6}$ (Figure 9). Figures 8 and 9, marked by (a), show curves for the ratio $E''/E' = 0.3$, (b) show curves for the ratio $E''/E' = 0.5$, and (c) show curves for the ratio $E''/E' = 0.7$.

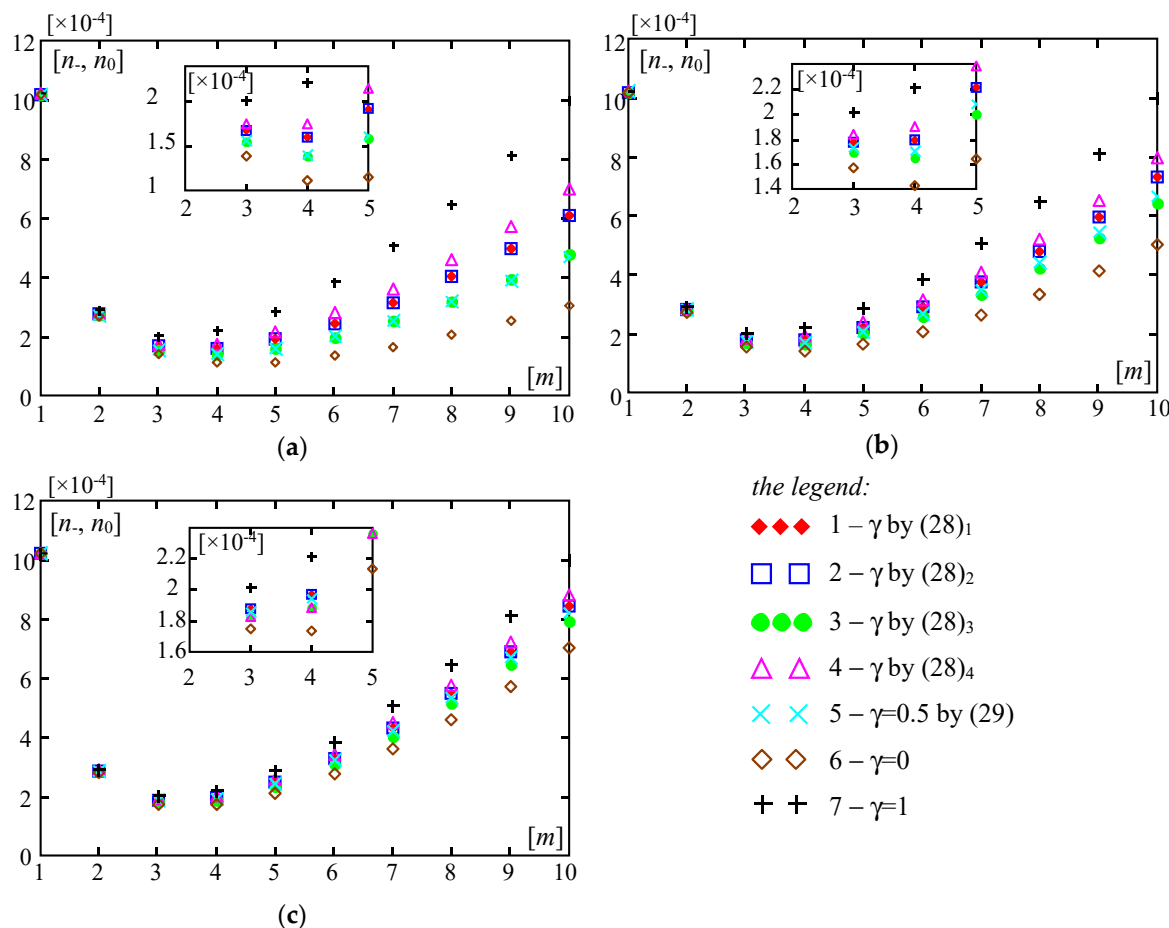


Figure 8. Values of dimensionless parameters n, n_0 of critical forces versus numbers of halfwaves of buckling m ($d/L = 0.01$, $l/L = 0.1$, $\kappa = 10^{-4}$): (a) For $E''/E' = 0.3$; (b) For $E''/E' = 0.5$; (c) For $E''/E' = 0.7$.

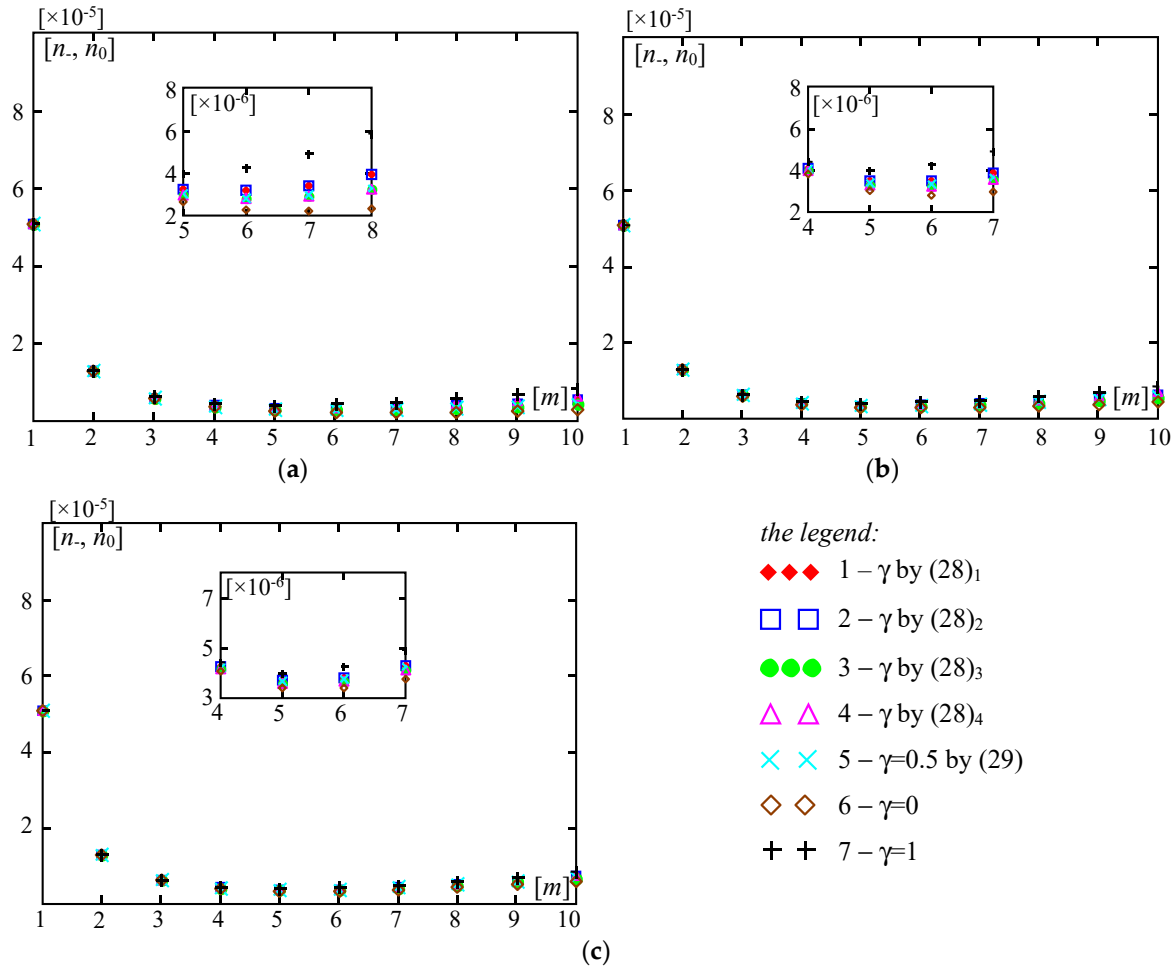


Figure 9. Values of dimensionless parameters n_- , n_0 of critical forces versus numbers of halfwaves of buckling m ($d/L = 0.002$, $l/L = 0.02$, $\kappa = 10^{-6}$): (a) $E''/E' = 0.3$; (b) $E''/E' = 0.5$; (c) $E''/E' = 0.7$.

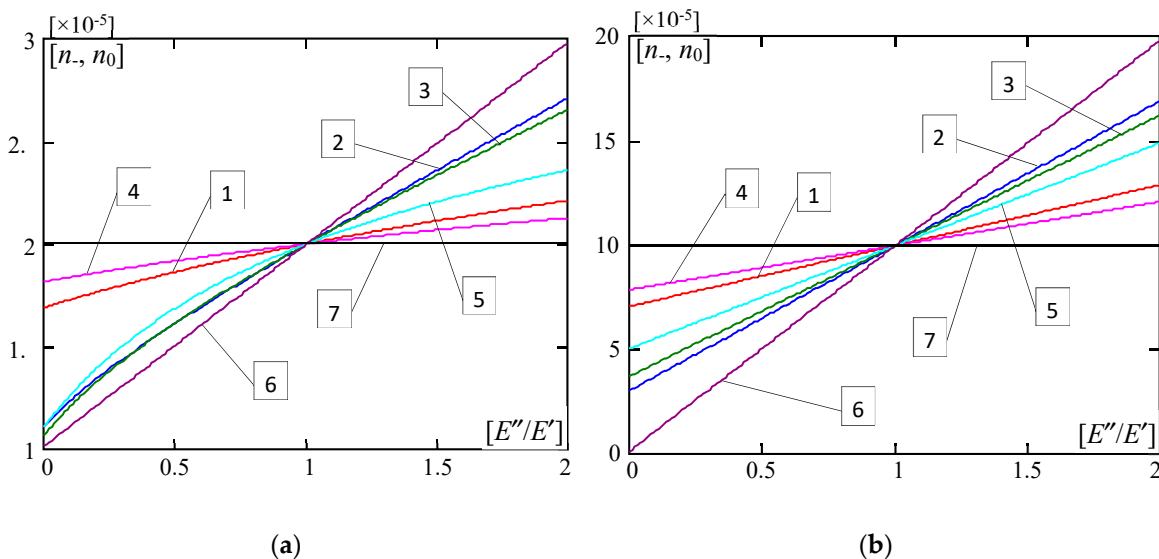


Figure 10. Values of dimensionless parameters n_- , n_0 of critical forces versus the ratio E''/E' ($l/L = 0.02$, $m = 1$): (a) $d/L = 0.01$, $\kappa = 10^{-6}$; (b) $d/L = 0.001$, $\kappa = 10^{-4}$. (1— γ by (28)₁, 2— γ by (28)₂, 3— γ by (28)₃, 4— γ by (28)₄, 5— γ by (29)).

Figure 10 presents plots of the dimensionless forces ratios n_-, n_0 versus the ratio $E''/E' \in (0,2]$. They are calculated for parameters: $l/L = 0.02$, $m = 1$. Figure 10 marked by (a) shows curves for $d/L = 0.01$, $\kappa = 10^{-6}$; but marked by (b) shows curves for $d/L = 0.001$, $\kappa = 10^{-4}$. Plots in Figure 10 numbered by 1–5 are related to microstructured plate bands described by the distribution functions of material properties $\gamma(x)$ defined by Equations (28) and (29). Moreover, curves numbered by 6 are made for the homogeneous plate band (with $\gamma = 0$, i.e., the plate band is made of the material with the Young's modulus E'') and by 7 for the homogeneous plate band (with $\gamma = 1$, i.e., the plate band is made of the material with the Young's modulus E').

4. Discussion

Analysing obtained numerical results presented in the above diagrams, it can be observed that differences between critical forces calculated by the tolerance model and by the asymptotic model are small for $d/L \geq 0.01$ (Figures 4 and 5). However, for $0.001 \geq d/L$ (Figures 6 and 7), differences between critical forces can be large. Moreover, these differences between the critical forces for various distribution functions of material properties are bigger for stiffer foundations, e.g., $\kappa = 10^{-4}$ (Figures 4a, 5a, 6a and 7a) than for softer foundations, e.g., $\kappa = 10^{-6}$ (Figures 4b, 5b, 6b and 7b).

In Figures 8 and 9, it is shown for what number m of halfwaves of buckling a critical force has the smallest value in relation to the distribution function of the material properties. It can be observed that the number m for the minimal critical force is related to the ratio E''/E' and distribution functions $\gamma(x)$ ((28), (29)).

For parameters $d/L = 0.01$, $l/L = 0.1$, $\kappa = 10^{-4}$ (cf. Figure 8) and for the ratio $E''/E' = 0.3$, the smallest critical forces for all considered distribution functions $\gamma(x)$ (28) and (29) and for the homogeneous plate band with $\gamma = 0$ (i.e., the material of the whole plate has the Young's modulus E'') are obtained for $m = 4$, but only for the homogeneous plate band with $\gamma = 1$ (i.e., the material of the whole plate has the Young's modulus E') the smallest critical force is for $m = 3$. For the ratio $E''/E' = 0.5$, the smallest critical forces for distribution functions $\gamma(x)$ (28)₃, (29) and for the homogeneous plate band with $\gamma = 0$ (i.e., the material of the whole plate has the Young's modulus E'') are obtained for $m = 4$, but for distribution functions $\gamma(x)$ (28)_{1,2,4} and the homogeneous plate band with $\gamma = 1$ (i.e., the material of the whole plate has the Young's modulus E') the smallest critical force is for $m = 3$. For the ratio $E''/E' = 0.7$, the smallest critical forces for all considered distribution functions $\gamma(x)$ (28) and (29) and for the homogeneous plate band with $\gamma = 1$ (i.e., the material of the whole plate has the Young's modulus E') are obtained for $m = 3$, but only for the homogeneous plate band with $\gamma = 0$ (i.e., the material of the whole plate has the Young's modulus E'') the smallest critical force is for $m = 4$.

For plate bands of smaller thickness, smaller basic cells, and softer foundation, i.e., for parameters: $d/L = 0.002$, $l/L = 0.02$, $\kappa = 10^{-6}$ (cf. Figure 9), and for the ratio $E''/E' = 0.3$, the smallest critical forces for all considered distribution functions $\gamma(x)$ (28) and (29) and for the homogeneous plate band with $\gamma = 1$ (i.e., the material of the whole plate has the Young's modulus E') are obtained for $m = 6$, but only for the homogeneous plate band with $\gamma = 0$ (i.e., the material of the whole plate has the Young's modulus E'') the smallest critical force is for $m = 7$. For the ratio $E''/E' = 0.5$, the smallest critical forces for distribution functions $\gamma(x)$ (28)₃, (29) and for the homogeneous plate band with $\gamma = 0$ (i.e., the material of the whole plate has the Young's modulus E'') they are obtained for $m = 6$, but for distribution functions $\gamma(x)$ (28)_{1,2,4} and the homogeneous plate band with $\gamma = 1$ (i.e., the material of the whole plate has the Young's modulus E') the smallest critical force is for $m = 5$. For the ratio $E''/E' = 0.7$ the smallest critical forces for all considered distribution functions $\gamma(x)$ (28) and (29) and for the homogeneous plate band with $\gamma = 1$ (i.e., the material of the whole plate has the Young's modulus E') are obtained for $m = 5$, but only for the homogeneous plate band with $\gamma = 0$ (i.e., the material of the whole plate has the Young's modulus E'') the smallest critical force is for $m = 6$.

From the results shown in Figure 10, it can be observed that values of dimensionless critical forces ratios for all microstructured plate bands fit between those specified for homogeneous plate bands with $\gamma = 0$ (i.e., the material of the whole plate has the Young's modulus E'') and with $\gamma = 1$

(i.e., the material of the whole plate has the Young's modulus E'). Linear plots of results are only for these two homogeneous plate bands. All other plots for microstructured plate bands are curvilinear, and it is more visible for thicker plates and a less rigid foundation (for e.g., $d/L = 0.01$, $\kappa = 10^{-6}$; cf. Figure 10a). Moreover, for the ratio $E''/E' > 1$ values of dimensionless critical forces ratios for all microstructured plate bands are bigger than these ratios for the homogeneous plate band with $\gamma = 1$ (i.e., the material of the whole plate has the Young's modulus E'), but smaller than these ratios for the homogeneous plate band with $\gamma = 0$ (i.e., the material of the whole plate has the Young's modulus E''). The descending order of values of these ratios for microstructured plate bands in relation to the distribution functions of properties $\gamma(x)$ is as follows: for $\gamma(x)$ by (28)₂, for $\gamma(x)$ by (28)₃, for $\gamma(x)$ by (29), for $\gamma(x)$ by (28)₁, for $\gamma(x)$ by (28)₄. However, for the ratio $E''/E' < 1$, these ratios for all microstructured plate bands are bigger than those for the homogeneous plate band with $\gamma = 0$, but smaller than those for the homogeneous plate band with $\gamma = 1$. The ascending order of values of these critical forces ratios for microstructured plate bands in relation to the distribution functions of properties $\gamma(x)$ is as follows: for $\gamma(x)$ by (28)₂, for $\gamma(x)$ by (28)₃, for $\gamma(x)$ by (29), for $\gamma(x)$ by (28)₁, for $\gamma(x)$ by (28)₄. However, it should be noted that for thicker plate bands and a softer foundation (for e.g., $d/L = 0.01$, $\kappa = 10^{-6}$; cf. Figure 10a), this order is disturbed, because for the ratio $E''/E' < 0.4$, values of these critical forces ratios for plate bands described by function $\gamma(x)$ by (28)₃ are bigger than those for function $\gamma(x)$ by (28)₂.

5. Conclusions and Remarks

Summarising considerations and obtained results, the following remarks can be formulated:

- The tolerance modelling approach allows us to replace differential equations of stability with non-continuous, tolerance-periodic, functional coefficients for microstructured functionally graded plates by differential equations with slowly-varying, smooth functional coefficients, which describe the effect of microstructure size on the overall behaviour of these plates.
- The governing equations of the tolerance model for the buckling of microstructured functionally graded plates leads to two formulas of critical forces—the lower fundamental critical force and the additional critical force, so-called the higher critical force.
- Values of the lower fundamental critical forces calculated by the tolerance model are almost the same as those obtained according to the asymptotic model (without the effect of microstructure), but slightly smaller.
- For very thin plate bands on a foundation, differences between the fundamental critical forces obtained in the framework of both the models—tolerance and asymptotic, grow strongly. However, it seems that one problem of this effect is still open.

The proposed tolerance model stands out among the models known from the literature in that it takes into account the effect of microstructure, and moreover, it describes the stability of thin plates with the functional gradation of properties (material and geometric) in the middle plane of the plate, resting on an elastic foundation. It seems appropriate to use this model further to solve specific problems. This study appears to be one of the first concerning the stability of the plates under consideration. In addition, it shows a certain versatility of the tolerance modelling method, which can be used not only in dynamic problems.

The above considerations do not close the subject. It appears that the considered problems will require further analysis, including when it comes to comparing the results obtained numerically or from experimental studies. Some validations of the tolerance model were done for dynamic problems using the finite element method, which was shown, among others in Reference [78] for thin functionally graded plates, and in Reference [72] for periodic Timoshenko beams. The analysis of additional (higher) critical force obtained under the tolerance model also remains open. An analysis of inverse problems will also be interesting in the future; for example, to design the distribution of different materials at the micro-level in order to obtain a specific behaviour of the considered plates.

Author Contributions: J.J. conceived and designed the tolerance and asymptotic models of thin functionally graded plates with a microstructure. M.K.-S. conceived and designed the tolerance and asymptotic models of buckling of thin functionally graded microstructured plates on an elastic foundation. M.K.-S. performed the calculation examples and analysis. J.J. and M.K.-S. made figures for paper, discussed obtained results and wrote the paper. All authors have read and agreed to the published version of the manuscript.

Funding: This research received no external funding.

Conflicts of Interest: The authors declare no conflict of interest.

Nomenclature

asymptotic model	
asymptotic modelling	
averaged Euler-Lagrange equations	
averaged lagrangean of plate, $\langle \Lambda_h \rangle$	
averaged part of in-plane forces, $N_{\alpha\beta}$	
averaging operator, $\langle \cdot \rangle$	
basic cell, Δ	
bending stiffnesses of plate, $d_{\alpha\beta}$	
dimensionless forces ratios, n_- , n_0	
dimensionless microstructure parameter, l/L	
distribution function of material properties, $\gamma(x)$	
effect of microstructure	
fluctuation amplitude, Q^A , Q	
fluctuation shape function, h^A , $h \in FS_\delta^\alpha(\Pi, \Delta)$	
functionally graded plate	
functionally graded structure	
higher critical force, N_+	
highly oscillating function, $HO_\delta^\alpha(\Pi, \Delta)$	
in-plane forces, $n_{\alpha\beta}$	
in-plane forces restriction	
lagrangean of plate, Λ	
lower critical forces, N_- , N_0	
macrodeflection, W	
micro-macro decomposition	
microstructure parameter, l	
oscillating part of in-plane forces, $\tilde{n}_{\alpha\beta}$	
periodic approximation (of function f), \tilde{f}	
plate midplane, Π	
Poisson's ratio of plate material, ν	
Ritz method	
slowly-varying function, $SV_\delta^\alpha(\Pi, \Delta)$	
stability of thin microstructured functionally graded plates on an elastic foundation	
thickness of plate, d	
thin microstructured functionally graded plate band	
thin microstructured functionally graded plates <i>aka</i> tolerance-periodic plates	
tolerance averaging approximation	
tolerance model	
tolerance modelling <i>aka</i> the tolerance averaging method	
tolerance parameter, δ	
tolerance-periodic function, $TP_\delta^\alpha(\Pi, \Delta)$	
tolerance-periodic structure	
Winkler's coefficient, k	
Young's modulus of plate material, E .	

References

1. Suresh, S.; Mortensen, A. *Fundamentals of Functionally Graded Materials*; The University Press: Cambridge, UK, 1998.
2. Woźniak, C.; Michalak, B.; Jędrysiak, J. (Eds.) *Thermomechanics of Heterogeneous Solids and Structures*; Łódź University of Technology: Łódź, Poland, 2008.
3. Bensoussan, A.; Lions, J.-L.; Papanicolaou, G. *Asymptotic Analysis for Periodic Structures*; North-Holland: Amsterdam, The Netherlands, 1978.
4. Kohn, R.V.; Vogelius, M. A new model for thin plates with rapidly varying thickness. *Int. J. Solids Struct.* **1984**, *20*, 333–350. [[CrossRef](#)]
5. Matysiak, S.J.; Nagórko, W. Microlocal parameters in the modelling of microperiodic plates. *Ing. Arch.* **1989**, *59*, 434–444. [[CrossRef](#)]
6. Batra, R.C.; Qian, L.F.; Chen, L.M. Natural frequencies of thick square plates made of orthotropic, trigonal, monoclinic, hexagonal and triclinic materials. *J. Sound Vib.* **2004**, *270*, 1074–1086. [[CrossRef](#)]
7. Królak, M.; Kowal-Michalska, K.; Mania, R.J.; Świński, J. Stability and load carrying capacity of multi-cell thin-walled columns of rectangular cross-sections. *J. Theor. Appl. Mech.* **2009**, *47*, 435–456.
8. Magnucka-Blandzi, E. Non-linear analysis of dynamic stability of metal foam circular plate. *J. Theor. Appl. Mech.* **2010**, *48*, 207–217.
9. Grygorowicz, M.; Magnucki, K.; Malinowski, M. Elastic buckling of a sandwich beam with variable mechanical properties of the core. *Thin-Walled Struct.* **2015**, *87*, 127–132. [[CrossRef](#)]
10. Wittenbeck, L.; Grygorowicz, M.; Paczos, P. Numerical analysis of sandwich beam with corrugated core under three-point bending. *AIP Conf. Proc.* **2015**, *1648*, 800007-1–800007-3. [[CrossRef](#)]
11. Grygorowicz, M.; Magnucka-Blandzi, E. Mathematical modeling for dynamic stability of sandwich beam with variable mechanical properties of core. *Appl. Math. Mech.* **2016**, *37*, 361–1374. [[CrossRef](#)]
12. Pawlus, D. Stability of Three-Layered Annular Plate with Composite Facings. *Appl. Compos. Mater.* **2017**, *24*, 141–158. [[CrossRef](#)]
13. Strek, T.; Jopek, H.; Fraska, A. Torsion of elliptical composite beams with auxetic phase. *Phys. Status Solidi* **2016**, *253*, 1359–1368. [[CrossRef](#)]
14. Jopek, H.; Strek, T. Torsion of a two-phased composite bar with helical distribution of constituents. *Phys. Status Solidi* **2017**, *254*. [[CrossRef](#)]
15. Aboudi, J.; Pindera, M.-J.; Arnold, S.M. Thermo-inelastic response of functionally graded composites. *Int. J. Solid Struct.* **1995**, *32*, 1675–1710. [[CrossRef](#)]
16. Aboudi, J.; Pindera, M.-J.; Arnold, S.M. A coupled higher-order theory for functionally graded composites with partial homogenization. *Compos. Eng.* **1995**, *5*, 771–792. [[CrossRef](#)]
17. Pindera, M.-J.; Dunn, P. Evaluation of the higher-order theory for functionally graded materials via the finite-element method. *Compos. Part B* **1997**, *28B*, 109–119. [[CrossRef](#)]
18. Aboudi, J.; Pindera, M.-J.; Arnold, S.M. Higher-order theory for functionally graded materials. *Compos. Part B* **1999**, *30*, 777–832. [[CrossRef](#)]
19. Goldberg, R.K.; Hopkins, D.A. Thermal analysis of a functionally graded material subject to a thermal gradient using the boundary element method. *Compos. Eng.* **1995**, *5*, 793–806. [[CrossRef](#)]
20. Martínez-Pañeda, M. On the finite element implementation of functionally graded materials. *Materials* **2019**, *12*, 287. [[CrossRef](#)]
21. Sofiyev, A.H.; Schnack, E. The stability of functionally graded cylindrical shells under linearly increasing dynamic torsional loading. *Eng. Struct.* **2004**, *26*, 1321–1331. [[CrossRef](#)]
22. Ferreira, A.J.M.; Batra, R.C.; Roque, C.M.C.; Qian, L.F.; Jorge, R.M.N. Natural frequencies of functionally graded plates by a meshless method. *Compos. Struct.* **2006**, *75*, 593–600. [[CrossRef](#)]
23. Bui, T.Q.; Khosravifard, A.; Zhang, C.; Hematiyan, M.R.; Golm, M.V. Dynamic analysis of sandwich beams with functionally graded core using a truly meshfree radial point interpolation method. *Eng. Struct.* **2013**, *47*, 90–104. [[CrossRef](#)]
24. Roque, C.M.C.; Ferreira, A.J.M.; Jorge, R.M.N. A radial basis function approach for the free vibration analysis of functionally graded plates using a refined theory. *J. Sound Vib.* **2007**, *300*, 1048–1070. [[CrossRef](#)]

25. Tornabene, F.; Liverani, A.; Caligiana, G. FGM and laminated doubly curved shells and panels of revolution with a free-form meridian: A 2-D GDQ solution for free vibrations. *Int. J. Mech. Sci.* **2011**, *53*, 443–470. [[CrossRef](#)]
26. Akbarzadeha, A.H.; Abbasib, M.; Eslami, M.R. Coupled thermoelasticity of functionally graded plates based on the third-order shear deformation theory. *Thin-Walled Struct.* **2012**, *53*, 141–155. [[CrossRef](#)]
27. Oktem, A.S.; Mantari, J.L.; Guedes Soares, C. Static response of functionally graded plates and doubly-curved shells based on a higher order shear deformation theory. *Eur. J. Mech. A/Solids* **2012**, *36*, 163–172. [[CrossRef](#)]
28. Tornabene, F.; Viola, E. Static analysis of functionally graded doubly-curved shells and panels of revolution. *Meccanica* **2013**, *48*, 901–930. [[CrossRef](#)]
29. Tornabene, F.; Fantuzzi, N.; Viola, E.; Batra, R.C. Stress and strain recovery for functionally graded free-form and doubly-curved sandwich shells using higher-order equivalent single layer theory. *Compos. Struct.* **2015**, *119*, 67–89. [[CrossRef](#)]
30. Tornebene, F.; Fantuzzi, N.; Bacciochi, M. On the mechanics of laminated doubly-curved shells subjected to point and line loads. *Int. J. Eng. Sci.* **2016**, *109*, 115–164. [[CrossRef](#)]
31. Ashoori, A.R.; Sadough Vanini, S.A. Thermal buckling of annular microstructure-dependent functionally graded material plates resting on an elastic medium. *Compos. Part B Eng.* **2016**, *87*, 245–255. [[CrossRef](#)]
32. Murin, J.; Aminbaghai, M.; Hrabovsky, J.; Kutiš, V.; Kugler, S. Modal analysis of the FGM beams with effect of the shear correction function. *Compos. Part B* **2013**, *45*, 1575–1582. [[CrossRef](#)]
33. Roque, C.M.C.; Martins, P.A.L.S.; Ferreira, A.J.M.; Jorge, R.M.N. Differential evolution for free vibration optimization of functionally graded nano beams. *Compos. Struct.* **2016**, *156*, 29–34. [[CrossRef](#)]
34. Jha, D.K.; Kant, T.; Singh, R.K. Free vibration response of functionally graded thick plates with shear and normal deformations effects. *Compos. Struct.* **2013**, *96*, 799–823. [[CrossRef](#)]
35. Sheikholeslami, S.A.; Saidi, A.R. Vibration analysis of functionally graded rectangular plates resting on elastic foundation using higher-order shear and normal deformable plate theory. *Compos. Struct.* **2013**, *106*, 350–361. [[CrossRef](#)]
36. Derras, M.; Kaci, A.; Draiche, K.; Tounsi, A. Non-linear analysis of functionally graded plates in cylindrical bending based on a new refined shear deformation theory. *J. Theor. Appl. Mech.* **2013**, *51*, 339–348.
37. Huangfu, Y.-G.; Chen, F.-Q. Single-pulse chaotic dynamics of functionally graded materials plate. *Acta Mech. Sin.* **2013**, *29*, 593–601. [[CrossRef](#)]
38. Fantuzzi, N.; Tornabene, F.; Viola, E.; Ferreira, A.J.M. A strong formulation finite element method (SFEM) based on RBF and GDQ techniques for the static and dynamic analyses of laminated plates of arbitrary shape. *Meccanica* **2014**, *49*, 2503–2542. [[CrossRef](#)]
39. Fantuzzi, N.; Tornabene, F. Strong Formulation Isogeometric Analysis (SFIGA) for laminated composite arbitrarily shaped plates. *Compos. Part B: Eng.* **2016**, *96*, 173–203. [[CrossRef](#)]
40. Liu, B.; Ferreira, A.J.M.; Xing, Y.F.; Neves, A.M.A. Analysis of composite plates using a layerwise theory and a differential quadrature finite element method. *Compos. Struct.* **2016**, *156*, 393–398. [[CrossRef](#)]
41. Kugler, S.; Fotiu, P.A.; Murin, J. The numerical analysis of FGM shells with enhanced finite elements. *Eng. Struct.* **2013**, *49*, 920–935. [[CrossRef](#)]
42. Tornabene, F.; Fantuzzi, N.; Bacciochi, M.; Viola, E.; Reddy, J.N. A numerical investigation on the natural frequencies of FGM sandwich shells with variable thickness by the local generalized differential quadrature method. *Appl. Sci.* **2017**, *7*, 131. [[CrossRef](#)]
43. Tornabene, F.; Bacciochi, M. Dynamic stability of doubly-curved multilayered shells subjected to arbitrarily oriented angular velocities: Numerical evaluation of the critical speed. *Compos. Struct.* **2018**, *201*, 1031–1055. [[CrossRef](#)]
44. Arefi, M.; Bidgoli, E.M.R.; Dimitri, R.; Bacciochi, M.; Tornabene, F. Application of sinusoidal shear deformation theory and physical neutral surface to analysis of functionally graded piezoelectric plate. *Compos. Part B Eng.* **2018**, *151*, 35–50. [[CrossRef](#)]
45. Arefi, M.; Bidgoli, E.M.R.; Dimitri, R.; Tornabene, F. Free vibrations of functionally graded polymer composite nanoplates reinforced with graphene nanoplatelets. *Aerosp. Sci. Technol.* **2018**, *81*, 108–117. [[CrossRef](#)]
46. Kołakowski, Z.; Mania, R.J. Dynamic response of thin FG plates with a static unsymmetrical stable postbuckling path. *Thin-Walled Struct.* **2015**, *86*, 10–17. [[CrossRef](#)]

47. Teter, A.; Mania, R.J.; Kołakowski, Z. Non-linear multi-mode buckling of non-symmetric FML/FGM thin-walled columns with open cross-sections under compression. *Compos. Struct.* **2017**, *167*, 38–49. [[CrossRef](#)]
48. Kołakowski, Z.; Mania, R.J. Influence of the coupling matrix B on the interactive buckling of FML-FGM columns with closed cross-sections under axial compression. *Compos. Struct.* **2017**, *173*, 70–77. [[CrossRef](#)]
49. Sadowski, T.; Burlayenko, V.N. Three-dimensional free vibration analysis of thermally loaded FGM sandwich plates. *Materials* **2019**, *12*, 2377. [[CrossRef](#)]
50. Cao, Z.; Liang, X.; Deng, Y.; Zha, X.; Zhu, R.; Leng, J. Novel semi-analytical solutions for the transient behaviors of functionally graded material plates in the thermal environment. *Materials* **2019**, *12*, 4084. [[CrossRef](#)]
51. Jafari, M.; Chaleshtari, M.H.B.; Abdolalian, H.; Craciun, E.; Feo, L. Determination of forces and moments per unit length in symmetric exponential FG plates with a quasi-triangular hole. *Symmetry* **2020**, *12*, 834. [[CrossRef](#)]
52. Qu, Z.; Cao, X.; Shen, X. Properties of Love waves in functional graded saturated material. *Materials* **2018**, *11*, 2165. [[CrossRef](#)]
53. Jha, D.K.; Kant, T.; Singh, R.K. A critical review of recent research on functionally graded plates. *Compos. Struct.* **2013**, *96*, 833–849. [[CrossRef](#)]
54. Brillouin, L. *Wave Propagation in Periodic Structures*; Dover Pub. Inc.: Dover, UK, 1953.
55. Wu, Z.-J.; Li, F.-M.; Wang, Y.-Z. Vibration band gap properties of periodic Mindlin plate structure using the spectral element method. *Meccanica* **2014**, *49*, 725–737. [[CrossRef](#)]
56. Zhou, X.Q.; Yu, D.Y.; Shao, X.; Wang, S.; Tian, Y.H. Band gap characteristics of periodically stiffened-thin-plate based on center-finite-difference-method. *Thin-Walled Struct.* **2014**, *82*, 115–123. [[CrossRef](#)]
57. Zhou, X.Q.; Yu, D.Y.; Shao, X.; Wang, S.; Zhang, S.Q. Simplified-super-element-method for analyzing free flexural vibration characteristics of periodically stiffened-thin-plate filled with viscoelastic damping material. *Thin-Walled Struct.* **2015**, *94*, 234–252. [[CrossRef](#)]
58. Cheng, Z.B.; Xu, Y.G.; Zhang, L.L. Analysis of flexural wave bandgaps in periodic plate structures using differential quadrature element method. *Int. J. Mech. Sci.* **2015**, *100*, 112–125. [[CrossRef](#)]
59. Woźniak, C.; Wierzbicki, E. Averaging Techniques in thermomechanics of composite solids. In *Tolerance Averaging Versus Homogenization*; Lodz University of Technology: Częstochowa, Poland, 2000.
60. Woźniak, C. (Ed.) *Mathematical Modelling and Analysis in Continuum Mechanics of Microstructured Media*; Publishing House of Silesian University of Technology: Gliwice, Poland, 2010.
61. Dell’Isola, F.; Rosa, L.; Woźniak, C. A micro-structural continuum modelling compacting fluid-saturated grounds. *Acta Mech.* **1998**, *127*, 165–182. [[CrossRef](#)]
62. Wierzbicki, E.; Woźniak, C. On the dynamics of combined plane periodic structures. *Arch. Appl. Mech.* **2000**, *70*, 387–398. [[CrossRef](#)]
63. Michalak, B. The meso-shape functions for the meso-structural models of wavy-plates. *ZAMM* **2001**, *81*, 639–641. [[CrossRef](#)]
64. Nagórko, W.; Woźniak, C. Nonasymptotic modelling of thin plates reinforced by a system of stiffeners. *Electr. J. Pol. Agric. Univ. Civ. Eng.* **2002**, *5*, 8p.
65. Baron, E. On dynamic behaviour of medium-thickness plates with uniperiodic structure. *Arch. Appl. Mech.* **2003**, *73*, 505–516. [[CrossRef](#)]
66. Jędrysiak, J. The length-scale effect in the buckling of thin periodic plates resting on a periodic Winkler foundation. *Meccanica* **2003**, *38*, 435–451. [[CrossRef](#)]
67. Mazur-Śniady, K.; Woźniak, C.; Wierzbicki, E. On the modelling of dynamic problems for plates with a periodic structure. *Arch. Appl. Mech.* **2004**, *74*, 179–190. [[CrossRef](#)]
68. Tomczyk, B. A non-asymptotic model for the stability analysis of thin biperiodic cylindrical shells. *Thin-Walled Struct.* **2007**, *45*, 941–944. [[CrossRef](#)]
69. Tomczyk, B. Dynamic stability of micro-periodic cylindrical shells. *Mech. Mech. Eng.* **2010**, *14*, 137–150.
70. Jędrysiak, J. Geometrically nonlinear vibrations of thin visco-elastic periodic plates on a foundation with damping: Non-asymptotic modelling. *J. Theor. Appl. Mech.* **2016**, *54*, 945–961. [[CrossRef](#)]
71. Domagalski, Ł.; Jędrysiak, J. Nonlinear vibrations of periodic beams. *J. Theor. Appl. Mech.* **2016**, *54*, 1095–1108. [[CrossRef](#)]

72. Domagalski, Ł.; Świątek, M.; Jędrysiak, J. An analytical-numerical approach to vibration analysis of periodic Timoshenko beams. *Compos. Struct.* **2019**, *211*, 490–501. [[CrossRef](#)]
73. Marczak, J.; Jędrysiak, J. Some remarks on modelling of vibrations of periodic sandwich structures with inert core. *Compos. Struct.* **2018**, *202*, 752–758. [[CrossRef](#)]
74. Jędrysiak, J.; Ostrowski, P. The effect of uncertain material properties on free vibrations of thin periodic plates. *Meccanica* **2017**, *52*, 3713–3730. [[CrossRef](#)]
75. Michalak, B.; Wirowski, A. Dynamic modelling of thin plate made of certain functionally graded materials. *Meccanica* **2012**, *47*, 1487–1498. [[CrossRef](#)]
76. Perliński, W.; Gajdzicki, M.; Michalak, B. Modelling of annular plates stability with functionally graded structure interacting with elastic heterogeneous subsoil. *J. Theor. Appl. Mech.* **2014**, *52*, 485–498.
77. Wirowski, A.; Michalak, B.; Gajdzicki, M. Dynamic modelling of annular plates of functionally graded structure resting on elastic heterogeneous foundation with two modules. *J. Mech.* **2015**, *31*, 493–504. [[CrossRef](#)]
78. Jędrysiak, J. Tolerance modelling of free vibration frequencies of thin functionally graded plates with one-directional microstructure. *Compos. Struct.* **2017**, *161*, 453–468. [[CrossRef](#)]
79. Kaźmierczak, M.; Jędrysiak, J. A new combined asymptotic-tolerance model of vibrations of thin transversally graded plates. *Eng. Struct.* **2013**, *46*, 322–331. [[CrossRef](#)]
80. Jędrysiak, J.; Kaźmierczak-Sobińska, M. On free vibration of thin functionally graded plate bands resting on an elastic foundation. *J. Theor. Appl. Mech.* **2015**, *53*, 629–642. [[CrossRef](#)]
81. Michalak, B. 2D tolerance and asymptotic models in elastodynamics of a thin-walled structure with dense system of ribs. *Arch. Civ. Mech. Eng.* **2015**, *15*, 449–455. [[CrossRef](#)]
82. Rabenda, M.; Michalak, B. Natural vibrations of prestressed thin functionally graded plates with dense system of ribs in two directions. *Compos. Struct.* **2015**, *133*, 1016–1023. [[CrossRef](#)]
83. Ostrowski, P.; Michalak, B. The combined asymptotic-tolerance model of heat conduction in a skeletal micro-heterogeneous hollow cylinder. *Compos. Struct.* **2015**, *134*, 343–352. [[CrossRef](#)]
84. Ostrowski, P.; Michalak, B. A contribution to the modelling of heat conduction for cylindrical composite conductors with non-uniform distribution of constituents. *Int. J. Heat Mass Transf.* **2016**, *92*, 435–448. [[CrossRef](#)]
85. Pazera, E.; Jędrysiak, J. Effect of microstructure in thermoelasticity problems of functionally graded laminates. *Compos. Struct.* **2018**, *202*, 296–303. [[CrossRef](#)]
86. Tomczyk, B.; Szczerba, P. Tolerance and asymptotic modelling of dynamic problems for thin microstructured transversally graded shells. *Compos. Struct.* **2017**, *162*, 365–373. [[CrossRef](#)]
87. Tomczyk, B.; Szczerba, P. Combined asymptotic-tolerance modelling of dynamic problems for functionally graded shells. *Compos. Struct.* **2018**, *183*, 176–184. [[CrossRef](#)]
88. Tomczyk, B.; Szczerba, P. A new asymptotic-tolerance model of dynamic and stability problems for longitudinally graded cylindrical shells. *Compos. Struct.* **2018**, *202*, 473–481. [[CrossRef](#)]



© 2020 by the authors. Licensee MDPI, Basel, Switzerland. This article is an open access article distributed under the terms and conditions of the Creative Commons Attribution (CC BY) license (<http://creativecommons.org/licenses/by/4.0/>).